



0017-9310(93)E0122-W

Natural convection above line heat sources in greenhouse canopies

M. AUBINET and J. DELTOUR

Faculté des Sciences Agronomiques, UER de Physique et Chimie Physique, Avenue de la Faculté 8,
B-5030 Gembloux, Belgium

(Received in final form 7 July 1993)

Abstract—The characteristics of a plume generated by natural convection above heating pipes in greenhouse row crops is studied. This plume differs from the free plume mainly in two respects: (i) owing to the particular geometry of the cell, a downward flow appears in the edges of the cell and interacts with the plume and (ii) owing to the presence of vegetation heat and momentum sinks appear in the cell crop. In consequence there is no conservation of heat and the evolution of the mass and momentum flows can be different according to the forces balance. An experimental study is first developed in which the air velocity and the temperature excess are measured. It shows that: (i) the similarity hypothesis is relevant in this case while the entrainment hypothesis is not, (ii) the decrease of excess temperature with height is steeper than in a free plume, and (iii) the air velocity increases (decreases) with height at low (high) heights. A theoretical model is also developed. It is based on the mass, momentum and heat transport equations and completed by three closure relations characterizing the drag, the lateral turbulent exchanges and the convective heat exchange with the leaves. The model makes it possible to relate the particular behaviour of the 'crop cell plume' to the presence of heat and momentum sinks in the cell crop. Its predictions are in good agreement with the measurements.

1. INTRODUCTION

1.1. Position of the problem

THE AIM of this work is to describe the aerodynamic movements in greenhouses of temperate areas during winter and spring. These movements are of great importance since they determine the characteristics of the microclimate in crops and hence the conditions of plant growth. In particular they control the removal of water vapour produced by the crop transpiration that has two implications; firstly, too high a humidity may induce diseases in the crop: moreover the plant-to-air-vapour pressure deficit determines the importance of the transpiration itself and so the health of the crop and finally the quality of the production. Secondly, the winter period is particularly crucial for horticulturists: production costs are higher and the added value of the production is the most important.

The most widespread type of winter culture under glass in northern Europe is a culture in lines (tomatoes or peppers) heated by pipes lying in the soil. The lines of vegetation—2–3 m high—can be as long as several tens of meters and are grouped in pairs (Fig. 1a), the pairs being separated from each other by a passage with heating pipes. These are the main heating devices in the greenhouse and, during cold periods, the only source of air movement in the crop. These movements are created by natural convection above the pipes. Under such conditions, it can be assumed that the greenhouse can be divided into a series of unconnected cells, each of them containing two lines of vegetation separated by a passage with heating lines (Fig. 1b),

and that the movements occur independently and identically in each cell. So it amounts to studying the characteristics of the plume induced by that type of heat source in a crop cell. We shall refer to this type of plume as the crop cell plume (CCP).

It is quite surprising that, in spite of their importance, the indoor air movements in a greenhouse were seldom studied and that the studies on greenhouse crop transpiration do not take them into account. The great difficulty of measuring and modelling them is probably the main reason of this omission. The theoretical and experimental studies closest to the CCP are those related to the two-dimensional (2D) turbulent free plume (FP). It was first investigated during the Second World War in Germany [1] and, independently, in Britain [2]. Further studies were developed more recently [3–6]. We shall recall here the main aspects of this theory.

1.2. Theoretical background: the free plume theory

The first feature of a free plume is the growth of its vertical mass flux with height: it results from the turbulent entrainment by the plume of air situated at its edges. The second one is the conservation of its vertical heat flux. Indeed, no heat exchange is carried along with the turbulent entrainment because the entrained air is not heated (its excess temperature is zero) and no other heat exchange can take place. Two hypotheses are required to close the problem: the first one states that horizontal distributions of vertical velocity and excess temperature keep the same shape

NOMENCLATURE

$a(z)$	crop leaf area density [$\text{m}^2 \text{m}^{-3}$]	w	vertical velocity [m s^{-1}]
a_0	regression parameter [equation (6)]	x	lateral position [m]
b, b_0	plume width [m]	z	vertical position [m].
c_d	drag coefficient	Greek symbols	
c_p	specific heat of the air [J kg^{-1}]	α	pipe heat transfer coefficients [$\text{W (m}^2 \text{K)}^{-1}$]
D	pipe diameter [m]	β	coefficient of thermal expansion of the air [K^{-1}]
DT	pipe-to-air temperature difference [K]	ΔT	temperature excess of the air [K]
d_f	equivalent leaflet length [m]	ε	pipe emissivity
f	profile function	ρ	air density [kg m^{-3}]
g	gravity acceleration [m s^{-2}]	σ	Boltzmann constant [$\text{W (m}^2 \text{K}^4)^{-1}$]
g_{BL}	leaf boundary layer conductance [m s^{-1}]	θ	general variable (represents vertical velocity or temperature excess) [m s^{-1}] or [K].
Gr	Grashof number	Subscripts	
k	von Kármán constant	c	related to convective exchange
l	mixing length [m]	0	axial value
n_θ	regression coefficient [equation (6)]	r	related to radiative exchange
Nu	Nusselt number	θ, w, t	related to general variable, vertical velocity, temperature excess, respectively.
p	air pressure [Pa]		
Q_l	linear heat power [W m^{-1}]		
R_{sq}	R square coefficient		
S_H	heat source per unit cell width in the crop [K s^{-1}]		
T_p, T_c, T_a	temperatures (of pipes, vegetation and air) [K]		
u	lateral velocity [m s^{-1}]		

at each height and heating power, the width of the distribution being in addition independent of the latter (similarity hypothesis); the second states that the lateral entrainment rate is proportional to the vertical mass flux at the same height (entrainment hypothesis). The proportionality constant is universal and is called the entrainment constant.

On these assumptions, the problem can be solved by giving the vertical profile of vertical velocity, excess temperature and width of the plume. The results show that at sufficiently large distances from the source the vertical velocity is constant with height, but the width of the plume increases linearly with it. This is in agreement with the growth of mass flow with height due to the entrainment. The assumptions also show that the excess temperature decrease needs to be in inverse proportion to the height in order to keep the vertical heat flux constant. Finally it is shown that the velocity and the excess temperature are increasing functions of the heating power.

1.3. Crop cell plume particularities

In spite of numerous similarities, the CCP and FP present differences that we shall detail below.

(a) *Doubling of the heat source.* The heating system in a CCP is made up by a pair of pipes while the FP theory takes into account one heat source line. The interaction between two sources has already been observed in the case of turbulent [7] and laminar [8] free plumes. These studies have shown that the

plumes, unable to entrain indefinitely the air set between each other, merged and performed rapidly like a single plume. So, at a sufficient distance from the sources, the results of the FP theory are suitable for a double plume provided a doubling of the heating power is taken into account. In our case we shall see that the merging of the plumes is already completed at 0.8 m (only 0.6 m above the sources). At this height, the horizontal distributions of velocity and excess temperature present a single maximum (Fig. 2).

(b) *Geometry of the cell.* A second difference between CCP and FP is due to the presence of adiabatic vertical limits that modify the geometry of the flow. The entrained air does not come from areas located around the plume at the same level, but from the top of the cell. This has two consequences: firstly the width of the ascending plume is limited by the presence of the downward flow and, secondly, at this boundary, interactions between the two flows can arise, in particular turbulent exchanges of heat or momentum can be induced between them. The hypothesis of cancelling of the turbulent fluxes at the edges of the plume, usual in the FP theory, cannot be used here.

On the other hand, the superior boundary (the roof of the greenhouse) does not play a significant role: it is more than 1 m higher than the crop cell top and a precedent study showed that the impact on the plume of a superior boundary was significant only when very close to it [9].

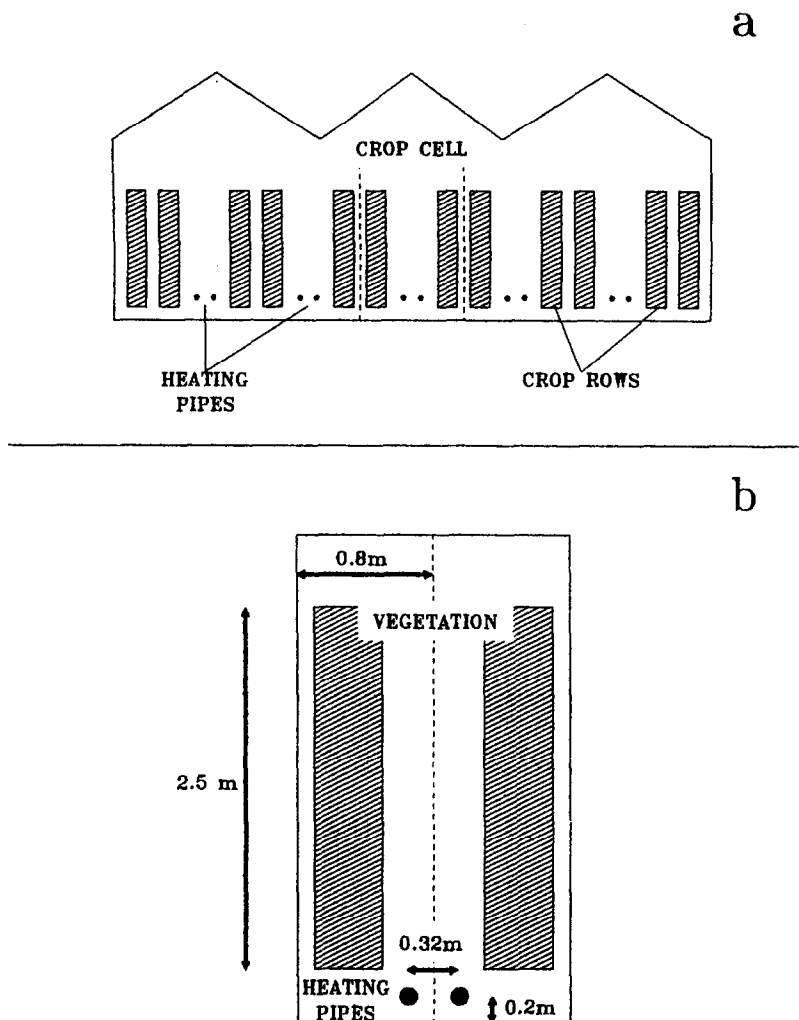


FIG. 1. Cross-sectional view of a typical northern European greenhouse (a) and of a 'crop cell' (b).

(c) *Vegetation.* The third difference with respect to the FP is the presence of vegetation at the edges of the plume that can play both a thermal and a mechanical role.

In heated greenhouses the vegetation is found to be most frequently cooler than the air [10–12]. It then acts like a heat sink for the plume and the conservation of the vertical heat flux can no longer be stated. That is the thermal effect.

The mechanical effect is multiple: vegetation may exert a drag on the ascending air, it may affect the turbulence at the edges of the plume and so act on the entrainment process and on the turbulent exchanges between upward and downward flows. Finally, it may canalize the flow owing to the particular row distribution of the vegetation.

In what follows we will study the characteristics of the upward flow in the crop cell. We first give experimental measurements of the vertical velocity and temperature excess in the cell and try to explain their behaviour. We then propose a theoretical model based on this explanation. A comparison between

measured and calculated values shows good agreement.

2. EXPERIMENTAL STUDY

2.1. Material and methods

Experimental device. The measurements are performed in a real culture set in an experimental greenhouse at the Faculté des Sciences Agronomiques in Gembloux (Belgium). A 2.5 m high, 4 m long and 1.6 m wide crop cell has been isolated. It consists of two 2.5 m high rows of vegetation (*Lycopersicon esculentum*, Mill.), separated by a passage in which heating pipes of 7 cm diameter have been laid at a distance of 0.32 m from each other. The temperature of the pipes, and hence the heating power, can be regulated. The cell has been isolated from the rest of the greenhouse by polyethylene screens to avoid disturbances from the inner air circulation.

All the measuring probes used during the experiment were realized and finalized at our department:

HORIZONTAL PROFILES

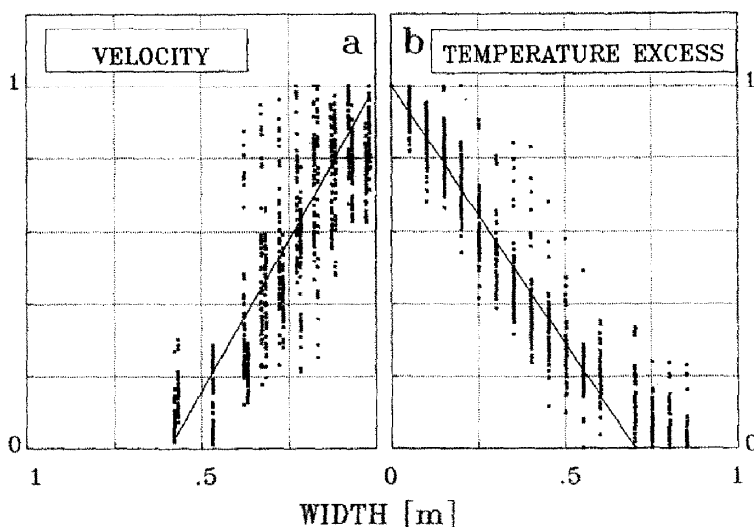


FIG. 2. Non-dimensional horizontal profiles (a) and temperature excesses (b) at 0.8 m height. The points indicate measured values and the solid lines the triangular theoretical profile.

the technical details related to these devices are given in other publications [13, 14].

The air temperature was measured by copper-constantan microthermocouples of very low thermal inertia. The movements of the air were measured by constant temperature thermistor anemometers. These devices, working on the same principle of the hot wire anemometer, have the advantage of being more economical, stable, resistant and consequently better adapted to a sustained utilization in a greenhouse. Their main weakness is the non-directionality of their response which leads to a bias when the flow is turbulent. A correction taking this error into account has been included with the measurements [14].

The pipe-to-air temperature difference (DT) is measured by means of a copper-constantan thermocouple. The linear heating power released by a couple of pipes is then deduced by

$$Q_l = 2\pi D(\alpha_r + \alpha_c)DT, \quad (1)$$

where the radiative transfer coefficient, α_r , is approximated by

$$\alpha_r = 4\sigma\epsilon T_p^3 \quad (2)$$

and the convective transfer coefficient is calculated, after [15], as

$$Nu = 0.48Gr^{0.25} \quad (3)$$

which describes the heat transfer between a horizontal cylinder and air for Grashof numbers lower than 10^{-9} , which is the case here. The factor 2 introduced in equation (1) takes into account the doubling of the heat sources. In what follows the linear heat flow will

always be expressed in watts per meter of crop cell.

Measurement process. The measurements of velocity and excess temperature were taken independently. The probes (amounting to 20) were arranged on a horizontal rail perpendicular to the heating pipes, 5 or 10 cm away from one another. Each series of measurements lasts for one night and is made at a fixed height. During this, the heat power increases from 0 to 360 W m^{-1} , and then decreases to zero. The measurements were taken by a programmable multimeter (FLUKE 8840A). They were collected, just as the values of DT , by a data logger finalized at our department and stored on a PC. We measured one horizontal profile every 10 s for the temperatures and every 20 s for the velocities.

Every 50 profiles, the mean of each measurement was calculated and stored. These means only will be used here. The profiles of the velocities have been measured at six different heights: 0.8, 1.1, 1.3, 1.5, 1.7 and 2.1 m. The profiles of the temperatures were measured at the four lowest heights only. Above 1.5 m the horizontal variations of temperature are no longer detectable since they are smaller than the measurement error.

Data treatment. To make a separate study of the horizontal distributions and the axial values of the variables possible, we introduce the following separation of variables:

$$\theta(x, z, Q_l) = \theta_0(x, z, Q_l) f_\theta(x, z, Q_l), \quad (4)$$

where θ is the value of the variable measured at position (z, x) ; θ_0 is the value of the variable on the axis at the same height; and f_θ is a non-dimensional

function characterizing the horizontal distribution of the variable.

In order to calculate the non-dimensional horizontal profile, any measurements affected by a large relative error were removed from the data (namely, entire profiles at heating powers less than 120 W m^{-1} and individual measurements taken further than 0.6 m away from the axis). Each profile was then centred individually on its maximal value and normalized by division by that value. A one-parameter, maximal on the axis profile function was fitted on each profile by means of a least squares method and the widths of all profiles were deduced; their dependence on heating power (similarity hypothesis) and height was tested.

The axial value of each profile was then calculated as a weighed mean of different measurements of the profile. The weighing factor is the value at x of the inverse of the profile function. Here again, low measurements (made at more than 0.4 m away from the axis) were removed to prevent an amplification of the measurement errors by the weighing.

2.2. Results

Horizontal profiles. The set of non-dimensional profiles measured at 0.8 m height is shown in Fig. 2 for velocity (Fig. 2a) and temperature excess (Fig. 2b). At this height, the plumes have merged: the horizontal profiles show a unique maximum located on the plume axis. The choice of the one-parameter maximal on the axis profile function is then suitable beyond this height. Several functions have been proposed in previous works: Gaussian [2, 3], Lorentzian [16] and top hat [6]. We have tested these three functions separately.

The top hat function was rapidly eliminated, giving too poor fittings. The Gaussian and Lorentzian functions gave reasonable fittings but were too sensitive to the measurements made in the wings of the profile, and as a consequence the distribution of the profile width shows artificial tendencies due to the relative errors on these measurements. This has already been pointed out by Rouse *et al.* [2], who specified that the Gaussian profile lost significance at large distances away from the plume axis. This is of course all the more the case in a laterally confined plume like the CCP.

Finally the only one-parameter function that provided a good fitting on the measurements and did not present these failures was the triangular function defined by

$$f_{\theta}(x, z, Q_i) = 1 - \frac{x}{b_{\theta}(x, Q_i)}, \quad (5)$$

where b_{θ} is the width of the profile.

At first sight, such a function looks unrealistic. It presents discontinuities and does not satisfy the zero slope condition on the axis and on the edges. However, these conditions are not essential for the resolution of the theoretical problem. Here, only the symmetry of

the profiles and the cancelling of the horizontal velocity on the axis are necessary. We chose, therefore, the triangular function to fit the horizontal profiles.

The mean value of the correlation coefficients in order to fit the triangular function on each horizontal profile is 0.926 for the excess temperatures and 0.794 for the velocities. In the two cases it shows evidence of the good quality of the fitting. The not so good value for the velocity profile is due to the greater error measurements leading to a greater dispersion of the results, as is apparent in Fig. 2.

We calculated the estimated value and confidence limits (confidence level = 0.95) of the regression coefficient of the profile width (related to a given height in order to avoid any interference caused by a possible dependence of the width on the height) according to the heating power and showed that it does not differ significantly from zero. Consequently the width can be supposed independent from the heating power. This is the similarity hypothesis.

In addition, we calculated the estimated values and confidence limits (confidence level = 0.95) of the width of the plume at each height; results are given in Fig. 3. The width varies between 0.6 and 1 m, but without any clear tendency. In particular no linear increase (as for the FP) can be inferred. This particular behaviour is probably due to the row structure of the vegetation. So the plume width is essentially a function of the space between the adjacent rows.

Axial values. The estimated values and confidence limits of the axial values of velocity and excess temperatures vs heating power are given for each height in Figs. 4 and 5. In imitation of the FP theory we can fit these measurements to a curvilinear relation of the type

$$\theta_0 = a_{\theta} Q_i^{n_{\theta}} \quad (6)$$

but this relation is not general as in FP: the values of the coefficients vary with the altitude. Their values as well as the R_{sq} of the regression are given in Table 1. Note the decrease with height of the quality of the regression of the temperature excess vs heat power. This is due to the growing incidence of the measurement error with height. The not so good value of R_{sq} for the velocity at the 1.5 m height is a consequence of a temporary failure of the material.

Using relations (6) and values of Table 1, it is possible to obtain an estimation of the excess temperature and the velocity at each investigated height for all values of the heating power. These estimations are given in Fig. 6.

It appears first (Fig. 6a) that the excess temperature decreases with height. In comparison with the prediction of the FP theory (lines in Fig. 6a), it is clear that the decrease is more important in the CCP, which confirms the existence of the heat sinks in a CCP. In Section 1.3 we identified two such sinks—the vegetation and the downward flow.

It also appears in Fig. 6(b) that the axial vertical velocity increases at lower heights and decreases at

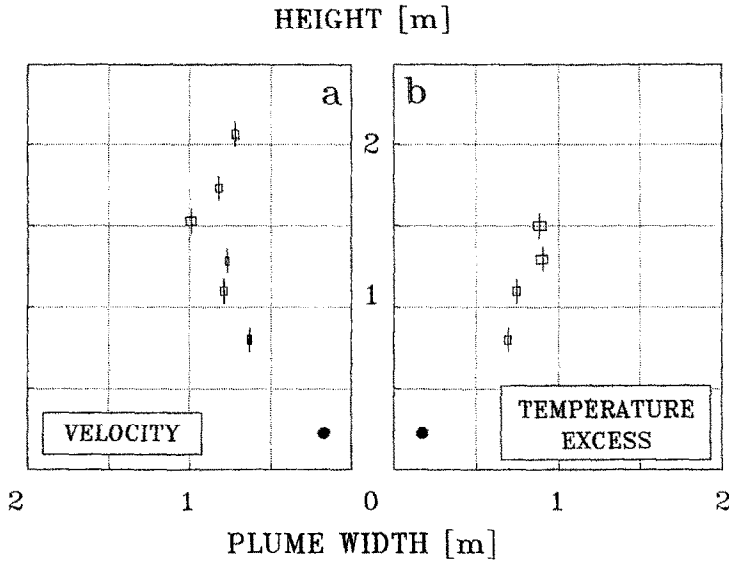


FIG. 3. Estimated value and confidence limits of the profile width at different heights for velocity (a) and temperature excess (b).

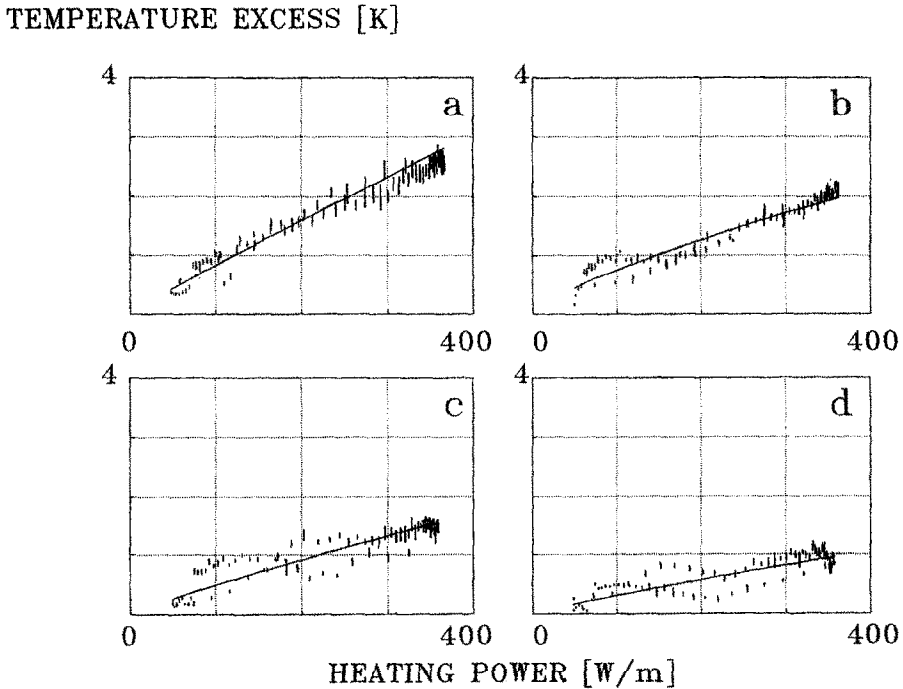


FIG. 4. Dependence of axial temperature excess on linear heating power at different heights: (a) 0.8 m, (b) 1.1 m, (c) 1.3 m, (d) 1.5 m.

higher heights (while the FP theory predicts no variation of velocity with height). This can be explained by the presence of opposing forces working on the ascending air. The buoyancy that accelerates the air upwards and, oppositely, the drag force and the turbulent lateral exchange of momentum that restrains it. At low altitudes, when the temperature excess is high, the first force prevails. The resulting increase of

mass and momentum flux leads to an increase of the vertical velocity owing to the canalization of the flow. At higher altitudes, the air having cooled down, the other forces prevail and a decrease in the vertical velocity is observed. The height at which the behaviour of the velocity reverse will be called the inversion height.

This inversion of behaviour of the vertical mass flux

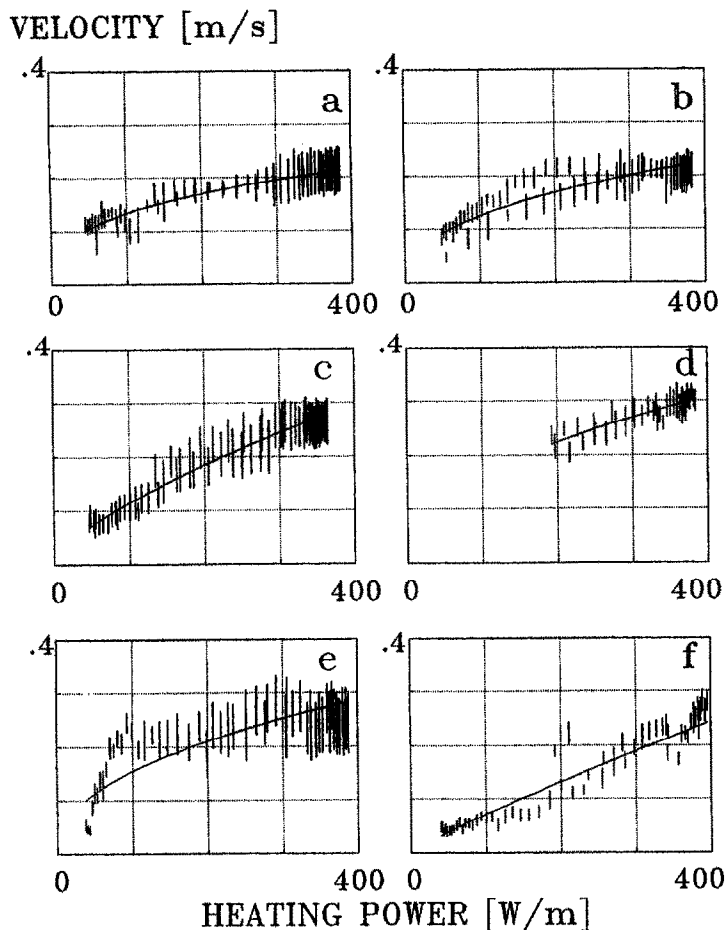


FIG. 5. Dependence of axial velocity on linear heating power at different heights: (a) 0.8 m, (b) 1.1 m, (c) 1.3 m, (d) 1.5 m, (e) 1.7 m, (f) 2.1 m.

Table 1. Values of the coefficients and R_{sq} of the regressions of temperature excess and velocity on linear heat power at different heights

Height	Temperature excess			Velocity		
	a_t	n_t	R_{sq}	a_u	n_u	R_{sq}
0.8	0.0112	0.928	0.936	0.0269	0.347	0.881
1.1	0.0239	0.749	0.832	0.0172	0.430	0.780
1.3	0.0080	0.897	0.752	0.0050	0.682	0.956
1.5	0.0051	0.892	0.645	0.0194	0.461	0.792
1.7	—	—	—	0.0201	0.444	0.626
2.1	—	—	—	0.0012	0.888	0.924

shows that the entrainment hypothesis is inconsistent in the CCP. The sign of the lateral to vertical mass fluxes ratio should be different below and above the inversion height. Of course in a CCP the turbulent entrainment is not only due to the upward flow but also depends on the vegetation and the downward flow.

We will now present a theoretical model that predicts the values of the vertical velocity and the tem-

perature excess in taking into account the particularities of the CCP.

3. MODEL

3.1. Fundamental equations

The basic equations are the equations of vertical turbulent transfer of mass (continuity equation), momentum (Reynolds equation) and heat [17]. For

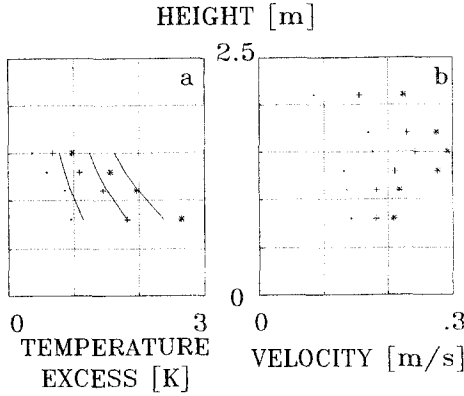


FIG. 6. Dependence of temperature excess (a) and axial velocity (b) on height at different linear heat powers. Estimations after relation (6) and results of Table 1 for $Q_0 = 120 \text{ W m}^{-1}$ (points), 240 W m^{-1} (crosses) and 360 W m^{-1} (asterisks). The solid line in (a) represents the predictions of the FP theory.

obvious symmetry reasons they are developed in a vertical plane perpendicular to the heating lines. In making assumptions of flow stationarity the system can be written as

$$\begin{aligned} \frac{\partial \bar{w}}{\partial z} + \frac{\partial \bar{u}}{\partial x} &= 0 \\ \bar{w} \frac{\partial \bar{w}}{\partial z} + \bar{u} \frac{\partial \bar{w}}{\partial x} &= \beta \overline{\Delta T} g - \frac{1}{\rho} \frac{\partial \bar{p}}{\partial z} - \frac{\partial}{\partial x} \overline{w'u'} \\ \bar{w} \frac{\partial \overline{\Delta T}}{\partial z} + \bar{u} \frac{\partial \overline{\Delta T}}{\partial x} &= \overline{S_H} - \frac{\partial}{\partial x} \overline{\Delta T' u'}. \end{aligned} \quad (7)$$

Here and below the overbars refer to a time mean and the primes to a fluctuation around the mean. The symbols are defined in the Nomenclature. The system (7) can be reduced to a system of differential equations after introducing of the horizontal distributions of velocities and excess temperatures (similarity hypothesis) and integration on the horizontal. If we adopt the triangular function and suppose in addition that its width is the same for velocity and excess temperature and for all heights (this seems quite reasonable according to the experimental results), the system is then

$$\begin{aligned} bI_1 \frac{d\bar{w}_0}{dz} &= -\bar{u}(z-b) & \text{I} \\ bI_2 \frac{d\bar{w}_0^2}{dz} &= bI_1 g \beta \Delta T_0 \\ & - \int_0^b \frac{1}{\rho} \frac{\partial \bar{p}}{\partial z} dx - \overline{w'u'}(z, b) & \text{IV} \\ & \text{III} \\ bI_2 \frac{d(\bar{w}_0 \Delta T_0)}{dz} &= \int_0^b \overline{S_H} dx - \overline{\Delta T' u'}(z, b), & \text{VI} \end{aligned} \quad (8)$$

where the normalization factors I_1 and I_2 are defined by

$$\begin{aligned} I_1 &= \int_0^b f_0(x) dx = \frac{1}{2} \\ I_2 &= \int_0^b f_0^2(x) dx = \frac{1}{3}. \end{aligned} \quad (9)$$

The 1/2 and 1/3 values of the normalization factors are due to the particular choice of the triangular function.

The first equation describes the mass flux evolution. It links its variations to lateral entrainment or rejection of air (I).

The second equation describes the momentum flux evolution. Three different terms contribute to it: the buoyancy (II), the pressure gradient force (III) (it was shown that [18], in a canopy, this term was at the origin of the drag force) and the lateral turbulent transfer term (IV). We have already noted that this term cannot be supposed to cancel out here owing to the presence of the vegetation and of the downward flow.

The third equation describes the heat flux evolution. Heat sinks are the vegetation (convective exchange, V) and the downward flow (lateral turbulent exchange, VI).

The system consists then in three equations with seven unknowns: the axial vertical velocity and temperature excess, the lateral horizontal velocity, the drag and turbulent forces, and the convective and turbulent heat fluxes. Four closure relations must be added for it to be solved.

3.2. Closure relations

Drag force. Numerous studies on the drag force show that this term could be expressed as [14]

$$\int_0^b \frac{1}{\rho} \frac{\partial \bar{p}}{\partial z} dx = bI_2 \bar{w}_0 a(z) C_d. \quad (10)$$

The leaf area density $a(z)$ depends on the type of culture and the species cultivated. In our case it was inferred from measurements of leaf area and internode length operated on 37 different plants at the end of the experiment. This profile is representative of the experimental condition because during the experiment the crop was fully developed and the profile of leaf area did not vary until the end of the experiment. A β -function was fitted to the measurements. The results of the measurements and the β -function are shown on Fig. 7.

The drag coefficient depends essentially on the geometry of the culture and of the leaves. Its value can be estimated by measurements taken in natural surroundings or in a wind tunnel [19–25]. Most values of this parameter are situated between 0.12 and 0.2. In our model, we will consider the drag coefficient as an adjustable parameter to be determined by fitting the model to the measurements.

Turbulent exchange terms. To parametrize the turbulent exchange terms, we will use a first-order closure

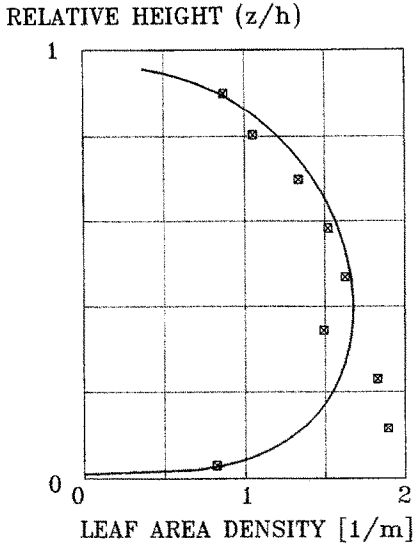


FIG. 7. Profile of leaf area density in a greenhouse crop (*Lycopersicon esculentum* Mill.). The points indicate measurements and the solid line $a(z) = 1.45z^{0.296}(h-z)^{0.436}$ (β -regression).

relation that links them to the horizontal mean concentration gradients

$$\overline{\theta'u'} = l^2 \left(\frac{d\bar{w}}{dx} \right) \left(\frac{d\bar{\theta}}{dx} \right), \tag{11}$$

where we introduce the mixing length. The validity of this relation in the case of open air canopies is questioned more and more. It has been shown [26] that the first-order closure relations are only valid while the scale of turbulence is smaller than the distance on which the gradient of concentration changes significantly. Although this condition is not met in an open-air crop, where most exchanges take place during gusts independent from the gradient of concentration [27], it might well be the case in a protected crop where such gusts do not exist and where the scale of turbulence is smaller. Pending a detailed investigation of turbulence in a greenhouse we shall use relation (11).

The problem is then to determine the mixing length in a canopy. In the case of homogeneous canopies Perrier [28] proposed to link this parameter to the leaf area density according to

$$l = \frac{k\pi}{2a(z)}. \tag{12}$$

Of course, the present situation differs notably from an open air homogeneous canopy. So it is not obvious that the relation (12) is well adapted to our problem. Consequently, we shall take the mixing length as an adjustable parameter. We have tested two different types of profiles of mixing length: a constant profile and a profile inversely proportional to the leaf area density according to Perrier's suggestion. As it is, the

latter allows the best fitting of the calculation to the measurements.

Convective heat exchange. Measurements of leaf-to-air temperature differences taken during the experimental phase of our work show that this quantity was rarely greater than 0.5 K, the air speed being currently greater than 0.2 m s^{-1} . The criterion commonly used to distinguish forced and free convection is given by the value of Gr/Re^2 [15]. In our case, it is rarely greater than 0.1 so that we can consider that the forced regime prevails. The heat convective heat exchange can be described by Fick's law

$$\rho C_p \int_0^b S_H dx = \rho C_p a(z) g_v b (T_v - T_a - I_1 \Delta T_0). \tag{13}$$

This relation takes into account the vertical gradient of temperature (the third term between parentheses) but neglects the horizontal heterogeneities in foliage or air temperatures and in leaf area index. The value of the leaf conductance equals twice the boundary layer conductance that can be calculated for the forced regime by [29]

$$g_v = 2g_{BL} = 2 \times (6.5 \times 10^{-3}) \left(\frac{\bar{u}}{d_f} \right)^{0.5} \tag{14}$$

that is adapted to real leaves. Let us recall, however, that this relation is empirical and that the quantity d_f is not the real length of the leaflet but an equivalent length close to it which also depends on the leaflet shape [30]. We shall therefore consider d_f as the third adjustable parameter of the model.

3.3. Solution and fitting

Equations (8) completed by the closure relations (10), (11) and (13) constitute a complete model. The unknowns are the axial vertical velocity and temperature excess and the lateral horizontal velocity. It can be solved if the boundary conditions are determined.

Two boundary conditions are necessary: the axial vertical velocity and the temperature excess at a 'departure height'. This is the lesser height in the crop cell where all the hypotheses underlying the model, in particular the hypothesis of similarity, are fulfilled. Our experimental results suggested we chose 0.8 m as the departure height. Note that, instead of this choice of boundary condition, the model is driven (indirectly) by the magnitude of the heating rate: indeed the axial vertical velocity and excess temperature at 0.8 m are exclusive functions of this variable (see Table 1). The model can be solved numerically; we used the Euler method improved by the prediction/correction procedure.

The form of the solution depends on the values of the three adjustable parameters: the drag coefficient of the leaves, the mixing length, and the equivalent leaflet length. The fitting of the model is realized after

Table 2. (A) Values of the adjustable parameters that give the best fitting of the model on experimental measurements. (B) Characteristics of the distributions of the measured-to-calculated differences for velocity and temperature excess

(A) Adjustable parameters	$C_d = 0$ $l = 0.39/a(z)$ $d_i = 0.10$ m	
(B)	Mean	Standard deviation
Velocity ($m\ s^{-1}$)	-0.0000	0.0260
Temperature excess (K)	-0.0511	0.0438

determination of the values of these parameters, which minimize the summed relative deviations, defined according to

$$\Delta rd = \frac{amd_w}{\Delta d_w} + \frac{amd_t}{\Delta d_t} \quad (15)$$

where *amds* are the absolute mean deviations between the calculated and measured values of velocity or excess temperature and *sds* are the standard deviations of velocity or excess temperature distributions.

The values of the parameters for which the best fitting is obtained are given in Table 2. This table also lists the mean and the standard deviation of the distributions of the measured-to-calculated differences of velocity and temperature excess. The very low values of this variable attests to the excellent quality of the fitting. The comparison between the measured and calculated values is given in Fig. 8.

4. DISCUSSION

The good agreement between measured and calculated values of the velocities and excess temperatures argues the validity of the CCP model. In particular, the predictions of the steeper decrease of

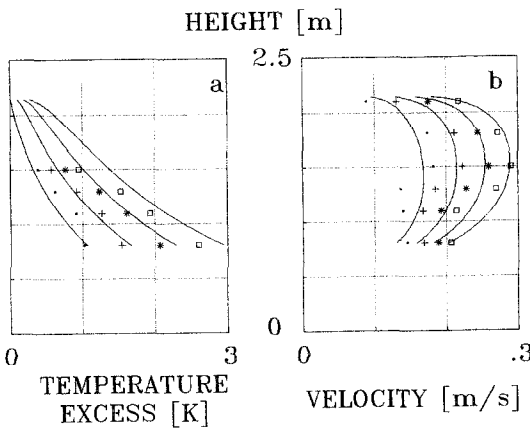


FIG. 8. Comparison between measured (points) and calculated (curves) values of axial velocity and temperature excess in the crop cell. The different curves and symbols correspond to linear heat fluxes of $100\ W\ m^{-1}$ (points); $200\ W\ m^{-1}$ (crosses); $275\ W\ m^{-1}$ (asterisks) and $350\ W\ m^{-1}$ (squares).

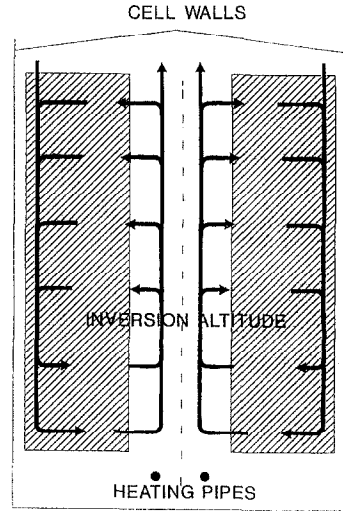


FIG. 9. Circulation induced by natural convection in the CCP.

the temperature excess than in the FP case (owing to heat losses) and of the inversion of the evolution of the vertical mass fluxes (owing to the inversion of the force balance) at the inversion height constitute an incontestable success.

In addition, agreement is reached for realistic values of two of the adjustable parameters: the equivalent length is close to the real length of tomato leaflets, the mixing length has the order of magnitude suggested by Perrier but is slightly lower. This could confirm the supposition made above that the scale of turbulence is weaker in a greenhouse than in open air.

The zero value of the drag coefficient is certainly the more surprising result. The model not being very sensitive to this parameter does not necessarily mean that the drag is exactly zero, but it suggests that the momentum loss is more likely due to the lateral turbulent exchange with downward flow than to the drag. This could be explained by the row structure of the culture: most of the air flow is found in the passage separating the plants where the drag effect is reduced. Considering the importance of the turbulent exchange term, further studies could be carried out with the object of improving knowledge of the turbulence in a greenhouse cell crop.

The results discussed here are relative to the axial vertical velocity and excess temperature. The first equation of the model allow us to extrapolate these results to the lateral mass fluxes. Under the inversion height, the growth of the vertical flux goes along with a lateral supply of mass to the plume: above it, its decrease goes along with a rejection of mass. An air circulation must be created inside the crop cell (Fig. 9). The air gets into the cell through the top of its lateral areas, it goes down, under the inversion height it is entrained by the ascending plume, and a part of the air is then rejected upward while another is rejected laterally and circulates again. As this type of circulation is carried out in the crop it may induce impor-

tant effects on the vegetation: if a part of the air circulates in the cell again, a stagnation of water vapour occurs and a microclimate can be created, characterized by a higher humidity which can be of great importance for the cultures. The relationship between the air circulation in the crop cell and the plant behaviour (its transpiration in particular) constitutes material for further research.

5. CONCLUSIONS

We studied the behaviour of a plume generated by natural convection above line heat sources in greenhouse row crops. This situation differs from the free plume mainly in two areas: (1) owing to the geometry of the cell crop a downward flow appears and interacts with the ascending plume. In consequence heat and momentum can be exchanged between the two flows by turbulence. And (2) the vegetation at the edges of the plume can constitute heat or momentum sinks: the heat can be exchanged by convection and the momentum by drag.

We first developed an experimental study of the plume and measured the velocities and temperature excesses for different heights and heat power in the crop cell. The main conclusions of the experiments are:

1. The similarity hypothesis, usual in the FP case, can also be applied in the CCP case.
2. The decrease of the excess temperature with height is steeper than in the FP case, which supports the hypothesis of the existence of heat sinks in the crop cell.
3. The vertical velocity increases at lower heights and decreases at higher heights. This can be explained by the action of opposing forces, some tending to accelerate the air upwards; some tending to restrain it.
4. In these conditions the entrainment hypothesis is inconsistent: according to the height it is lower or higher than the inversion height; air can be entrained or rejected.

We developed then a theoretical model that is based on the same equations as the free plume models but takes into account the presence of heat and momentum sinks. Four closure relations are introduced to parametrize these sinks. The model is solved and fitted on measurements. We found that:

1. There is a very good agreement between modelled and measured values of velocities and excess temperatures. In particular, the steeper decrease of temperature excess and the versatile behaviour of the velocity are well reproduced by the model.
2. Best fitting is obtained for realistic values of the parameters driving the turbulent exchanges and the convective heat flux.
3. The momentum losses by drag seem to be prac-

tically negligible. However this last conclusion needs to be confirmed by a deeper analysis.

4. An extrapolation of the model by use of the continuity equation suggests that CCP generates in the crop cell a circulation of air: a part of the air of the plume can be brought again into circulation in the crop cell which induces a stagnation in the crop of the water vapour transpired by the vegetation. The impact of this circulation on the transpiration of the crop is of great importance for the plant quality and can constitute the subject of further studies.

REFERENCES

1. W. Schmidt, Turbulente Ausbreitung eines Stromes eritzter Luft. 1 Teil. *Z. Angew. Math. Mech.* **21**, 265–278 (1941).
2. H. Rouse, C. S. Yih and H. W. Humphreys, Gravitational convection from a boundary source. *Tellus* **4**, 202–210 (1952).
3. S. L. Lee and H. W. Emmons, A study of natural convection above a line fire. *J. Fluid Mech.* **11**, 353–368 (1961).
4. N. Kotsovinos and E. J. List, Plane turbulent buoyant jets. Part 1: integral properties. *J. Fluid Mech.* **81**, 25–44 (1977).
5. M. R. Malin, The decay of mean and turbulent quantities in vertical forced plumes. *Appl. Math. Modelling* **11**, 301–314 (1987).
6. J. S. Turner, *Buoyancy Effects in Fluids*. Cambridge University Press, Cambridge (1959).
7. H. Rouse, W. D. Baines and H. W. Humphreys, Free convection over parallel sources of heat. *Proc. Phys Soc.* **B66**, 393–399 (1952).
8. L. Pera and B. Gebhart, Laminar plumes interactions. *J. Fluid Mech.* **68**, 259–271 (1975).
9. W. D. Baines and J. S. Turner, Turbulent convection from a source in a confined region. *J. Fluid Mech.* **37**, 51–80 (1969).
10. I. Seginer, On the night transpiration of greenhouse roses under glass or plastic cover. *Agric. For. Meteorol.* **30**, 257–268 (1984).
11. X. Yang, T. H. Short, R. D. Fox and W. L. Bauerle, Transpiration, leaf temperature and stomatal resistance of a greenhouse cucumber crop. *Agric. For. Meteorol.* **51**, 197–209 (1990).
12. L. Zhang and R. Lemeur, Effect of aerodynamic resistance on energy balance and Penman–Monteith estimates of evapotranspiration in greenhouse conditions. *Agric. For. Meteorol.* **58**, 229–240 (1992).
13. M. Aubinet, Transports de chaleur et de vapeur d'eau dans les couverts végétaux sous serre: approche théorique et expérimentale. Ph.D. dissertation, Gembloux (1991).
14. M. Aubinet, M. Yernaux and J. Deltour, Mise au point et étalonnage d'anémomètres thermiques pour la mesure de faibles vitesses d'écoulement d'air. *J. Phys III France* **2**, 2397–2409 (1992).
15. J. Monteith, *Principles of Environmental Physics*. Edward Arnold, London (1973).
16. B. Guillou, M. Brahimi and Doan Kim Son, Structure turbulente d'un panache thermique. Aspect dynamique. *J. Méc. Th. Appl.* **5**, 371–401 (1986).
17. A. S. Monin and A. M. Yaglom, *Statistical Fluid Dynamics*. MIT Press, Cambridge, MA (1971).
18. M. R. Raupach and A. S. Thom, Turbulence in and above plant canopies. *Ann. Rev. Fluid Mech.* **13**, 97–129 (1981).
19. G. B. K. Baines, Turbulence in a wheat crop. *Agric. Meteorol.* **10**, 93–105 (1972).

20. D. Baldocchi, Mass and energy exchanges of soybeans : microclimate-plant architectural interactions. Ph.D. thesis, University of Nebraska, Lincoln (1982).
21. G. den Hartog and R. H. Shaw, A field study of atmospheric exchanges processes within a vegetative canopy. In *Heat and Mass Transfer in the Biosphere* (Edited by de Vries and Afgan), pp. 299-309. John Wiley, New York (1975).
22. J. J. Landsberg and G. B. James, Wind profiles in plant canopies. Studies of an analytical model. *J. Appl. Ecol.* **8**, 729-741 (1971).
23. I. Seginer, P. J. Mulhearn, E. F. Bradley and J. J. Finnigan, Turbulent flow in a model plant canopy. *Bound. Layer Meteorol.* **10**, 423-453 (1976).
24. Z. Uchijima and J. L. Wright, An experimental study of air flow in a corn plant-air layer. *Bull. Nat. Inst. Agric. Sci. Japan* **A11**, 19-65 (1964).
25. N. R. Wilson and R. H. Shaw, A higher order closure model for canopy flow. *J. Appl. Meteorol.* **16**, 1197-1205 (1977).
26. S. Corrsin, Limitation of gradient transport models in random walks in turbulence. *Adv. Geophys.* **18A**, 25-60 (1974).
27. O. T. Denmead and E. F. Bradley, On scalar transports in plant canopies. *Irrig. Sci.* **8**, 131-149 (1987).
28. A. Perrier, Etude et essai de modélisation des échanges de masse et d'énergie au niveau des couverts végétaux. Doctoral thesis, University of Paris VI, INRA (1974).
29. J. J. Finnigan and M. R. Raupach, Transfer processes in plant canopies in relation to stomatal characteristics. In *Stomatal Function* (Edited by E. Zeiger, G. D. Farquar and I. R. Cowan), pp. 385-430. Stanford University Press, Stanford, CA (1987).
30. D. F. Parkhurst, P. R. Duncan, D. M. Gates and F. Kreith, Wind-tunnel modelling of convection of heat between air and broad leaves of plants. *Agric. Meteorol.* **5**, 33-47 (1969).